REPORT DOCUMENTATION PAGE

Form Approved OMB NO. 0704-0188

The public reporting burden for this collection of information is estimated to average 1 hour per response, including the time for reviewing instructions, searching existing data sources, gathering and maintaining the data needed, and completing and reviewing the collection of information. Send comments regarding this burden estimate or any other aspect of this collection of information, including suggesstions for reducing this burden, to Washington Headquarters Services, Directorate for Information Operations and Reports, 1215 Jefferson Davis Highway, Suite 1204, Arlington VA, 22202-4302. Respondents should be aware that notwithstanding any other provision of law, no person shall be subject to any oenalty for failing to comply with a collection of information if it does not display a currently valid OMB control number.
PLEASE DO NOT RETURN YOUR FORM TO THE ABOVE ADDRESS.

1. REPORT DATE (DD-MM-YYYY)	2. REPORT TYPE	3. DATES COVERED (From - To)
28-09-2018	Final Report	1-Sep-2015 - 31-May-2016

4. TITLE AND SUBTITLE

Final Report: Discovering High Intensity Room Temperature Visible Spectrum Piezoluminescence in Self-Assembled Grain-Oriented Hierarchical Multilayers (Topic 9.1 Materials by Design; TPOC John Prater)

5a. CONTRACT NUMBER

W911NF-15-1-0520

5b. GRANT NUMBER

5c. PROGRAM ELEMENT NUMBER

611102

6. AUTHORS

5d. PROJECT NUMBER

5e. TASK NUMBER

5f. WORK UNIT NUMBER

7. PERFORMING ORGANIZATION NAMES AND ADDRESSES

Virginia Polytechnic Institute & State Unive
North End Center, Suite 4200
300 Turner Street, NW
Blacksburg, VA 24061 -0001

8. PERFORMING ORGANIZATION REPORT NUMBER

9. SPONSORING/MONITORING AGENCY NAME(S) AND ADDRESS (ES)

U.S. Army Research Office
P.O. Box 12211
Research Triangle Park, NC 27709-2211

10. SPONSOR/MONITOR'S ACRONYM(S)

ARO

11. SPONSOR/MONITOR'S REPORT NUMBER(S)

66199-MS-II.2

12. DISTRIBUTION AVAILIBILITY STATEMENT

Approved for public release; distribution is unlimited.

13. SUPPLEMENTARY NOTES

The views, opinions and/or findings contained in this report are those of the author(s) and should not contrued as an official Department of the Army position, policy or decision, unless so designated by other documentation.

14. ABSTRACT

15. SUBJECT TERMS

16. SECURITY CLASSIFICATION OF:			17. LIMITATION OF ABSTRACT	15. NUMBER OF PAGES	19a. NAME OF RESPONSIBLE PERSON
a. REPORT	b. ABSTRACT	c. THIS PAGE			Yongke Yan
UU	UU	UU	UU		19b. TELEPHONE NUMBER 540-558-8088

RPPR Final Report
as of 03-Oct-2018

Agency Code:

Proposal Number: 66199MSII **Agreement Number: W911NF-15-1-0520**
INVESTIGATOR(S):

Name: Yongke Yan
Email: yanthu@vt.edu
Phone Number: 5405588088
Principal: Y

Organization: **Virginia Polytechnic Institute & State University**
Address: North End Center, Suite 4200, Blacksburg, VA 240610001
Country: USA
DUNS Number: 003137015 EIN: 546001805
Report Date: 31-Aug-2016 Date Received: 28-Sep-2018
Final Report for Period Beginning 01-Sep-2015 and Ending 31-May-2016
Title: Discovering High Intensity Room Temperature Visible Spectrum Piezoluminescence in Self-Assembled Grain-Oriented Hierarchical Multilayers (Topic 9.1 Materials by Design; TPOC John Prater)
Begin Performance Period: 01-Sep-2015 **End Performance Period:** 31-May-2016
Report Term: 0-Other
Submitted By: Yongke Yan Email: yanthu@vt.edu
Phone: (540) 558-8088
Distribution Statement: 1-Approved for public release; distribution is unlimited.

STEM Degrees: 0 **STEM Participants:** 0

Major Goals: Piezoluminescence (PL) implies generation of luminescence in the visible spectrum by mechanical action. The effect allows direct conversion of mechanical stress into light and has been observed in compounds with suitable crystallographic symmetry modified with activator ion. The mechanism behind the emission has been proposed to be as follows: (i) application of stress produces local electric field in the material due to the piezoelectric effect and the magnitude of field is significantly high in the vicinity of the activator ion due to local structural distortion; (ii) local field due to piezoelectric effect may result in reducing the trap-depth of the carriers or it may cause the band bending; (iii) next thermal detrapping or charge tunnel can occur; and (iv) lastly, generation of the excitor ions and their de-excitations results in the PL effect. The underlying basis for the effect thus lies in the presence of the local piezoelectricity and energy states available from the suitable activator ion. In this program, we utilized the advances made in the understanding of ceramic nanocomposites and coupled it with the fundamentals behind the PL emission to realize a hierarchical structure with high intensity room temperature emission. The focus in this effort was on establishing the structure – property – performance relationships governing the interactions between the stress, crystallography, microstructure and light emission. PL can be utilized in various scenarios where mechanical energy is continuously available surfaces of the aircrafts, automobiles and ships; roadways and pedestrian walkways; high deformation structures such as windmills and flexible rooftops, etc. New sensing technologies for stress, impact, and damage could be designed based on the PL effect. The effect could also be used for visualization of stress propagation in structures such as pipes and mounts. Recently, a safety management system was proposed where PL-sensor emits light in response to mechanical stress which is detected by the image sensing nodes that wirelessly communicate with the centralized system. The non-contact part of this system, since light is used for detection and communication, is highly attractive. Further, the stress sensing is passive as PL sensor responds directly by emitting light in response to the mechanical stimulation.

Accomplishments: See attached PDF file.

Training Opportunities: Two postdoctoral fellows were trained during the course of this program. This included opportunities for providing lecture, mentoring students, discussions with sponsors, and writing whitepapers. Upon completion, one of the postdoc has moved to industry position and other has accepted faculty position at Penn State. Thus, both the postdocs were successfully transitioned in their careers.

RPPR Final Report
as of 03-Oct-2018

Results Dissemination: One journal paper was published during the course of this program:

Jiayong Gan, Min Gyu Kang, Michael A Meeker, Fiti A. Khodaparast, Robert J. Bonnar, James E. Mahaney, Deepam Maurya, and Shashank Priya, “Enhanced piezoluminescence in non-stoichiometric ZnS:Cu microparticle based light emitting elastomers” Journal of Materials Chemistry C, Vol. 5, 5387 (05/12/2017)

Further, postdoctoral fellows presented the results from this program at Industry Advisory Board meeting of Center for Energy Harvesting Materials and Systems.

Honors and Awards: Nothing to Report

Protocol Activity Status:

Technology Transfer: We are having discussions with Radiant Technology on developing health monitoring sensors using PL phenomenon. Presentations were made to the president of company and he expressed interest in pursuing to implement this material.

We have initiated collaboration on PZL particles and composite processing technique with Dr. Wetzel at Army Research Laboratory (ARL) for developing novel PZL optical fiber. See details in the attached PDF file.

PARTICIPANTS:

Participant Type: Postdoctoral (scholar, fellow or other postdoctoral position)
Participant: Jiayong Gan
Person Months Worked: 6.00 **Funding Support:**
Project Contribution:
International Collaboration:
International Travel:
National Academy Member: N
Other Collaborators:

Participant Type: Postdoctoral (scholar, fellow or other postdoctoral position)
Participant: Min Gyu Kang
Person Months Worked: 3.00 **Funding Support:**
Project Contribution:
International Collaboration:
International Travel:
National Academy Member: N
Other Collaborators:

ARTICLES:

RPPR Final Report
as of 03-Oct-2018

Publication Type: Journal Article Peer Reviewed: Y **Publication Status:** 1-Published
Journal: Journal of Materials Chemistry C
Publication Identifier Type: DOI Publication Identifier: 10.1039/C7TC01146F
Volume: 5 Issue: 22 First Page #: 5387
Date Submitted: 9/28/18 12:00AM Date Published:
Publication Location:
Article Title: Enhanced piezoluminescence in non-stoichiometric ZnS:Cu microparticle based light emitting elastomers
Authors: Jiayong Gan, Min Gyu Kang, Michael A. Meeker, Giti A. Khodaparast, Robert J. Bodnar, James E. Maha
Keywords: Piezoluminescence, piezoelectric, zinc sulphide, light emission, spectroscopy
Abstract: Piezoluminescence (PZL), also referred to as mechanoluminescence (ML), is a promising energy conversion mechanism for realizing mechanically driven photon sources including handheld displays, lighting, bioimaging and sensing applications. However, the realization of a visible PZL intensity at room temperature from low mechanical stresses has been fundamentally challenging. Herein, we describe a PZL elastomer exhibiting significantly enhanced brightness under ambient conditions. The elastomer consisted of defect-engineered non-stoichiometric Cu-doped ZnS (ZnS:Cu) microparticles in a polydimethylsiloxane (PDMS) matrix. The role of the defect structure was found to be the controlling parameter in the nature of PZL emission. Hydrogenation treatment was designed to induce a controlled concentration of sulfur vacancies that provided the trapped electrons, which had a strong correlation with the PZL performance of ZnS:Cu.
Distribution Statement: 1-Approved for public release; distribution is unlimited.
Acknowledged Federal Support: **Y**

Final Progress Report

1. Statement of the problem studied

Piezoluminsecence (PZL) refers to the light emission induced by mechanical stress. PZL is a promising energy conversion phenomena that will enable high resolution dynamic stain sensing[1], novel display devices[2, 3], bio imaging[4], artificial skin[5], *etc*. However in literature, PZL effect has been considered as a secondary effect and enhancing PZL intensity has not been a major research focus because of the complexity in directly integrating with the practical applications. We have demonstrated flexible and durable PZL rubber with high intensity light emission using ZnS:Cu material, which has an outstanding PZL performance. The ZnS:Cu system is well-known as electroluminescence material and is currently utilized as phosphor in displays and light sources. ZnS:Cu exhibits finite piezoelectricity, which allows it to generate electric potential under applied stress and strain. Coupling between electroluminescence and piezoelectric properties is the main driving force for the PZL effect in ZnS:Cu system. Copper doping induces trapped electrons in the donor state and trapped holes in the acceptor state. Under applied mechanical stress, the conduction and valence bands of ZnS are tilted due to the piezoelectric potential. As a result, the trapped electrons are detrapped into the conduction band where recombination occurs with light emission (Figure 1). Thus, the intensity of the emitted light strongly depends on the defect structure of the material and the external stress induced internal piezoelectric field. In this project, we have performed intensive study to enhance the emitted light intensity through defect engineering and optimization of mechanical properties of the flexible PZL composite. In parallel, we have explored various applications using developed PZL elastomers, such as optical fiber composite, which is one of the promising strain/damage detection component, PZL gloves, and writing tracker.

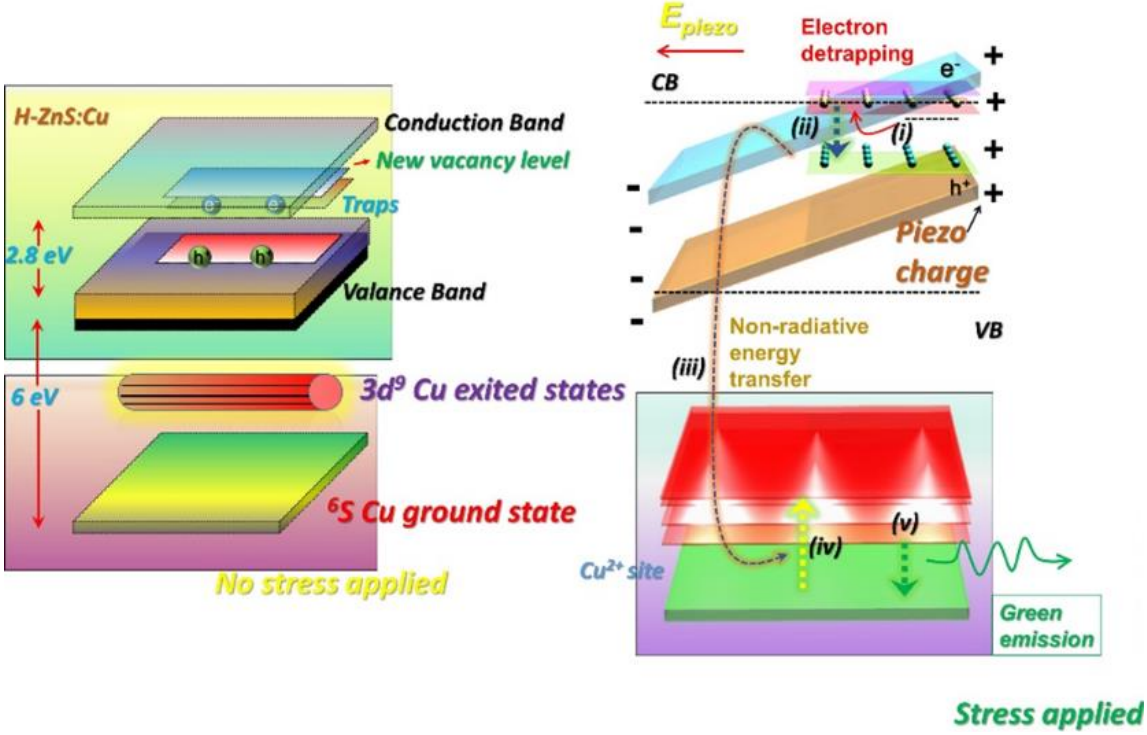

Figure 1. Mechanism for inducing PZL. Schematic illustration of band diagram of H-ZnS:Cu under zero stress (left). The PZL effect initiates the emission process under stress (right).

2. Summary of the most important results

(a) <u>*Defect engineering* –</u> In order to enhance the light emission intensity in ZnS:Cu material, we have controlled the donor densities resulting from introduction of sulfur vacancies *via* thermal treatment in hydrogen atmosphere. We have developed a facile controllable method to synthesize H-ZnS:Cu microparticles that possess different amounts of sulfur vacancies by hydrogenation treatment. ZnS:Cu is a ceramic material and inherently very brittle under stress. In order to

overcome this challenge, we dispersed H-ZnS:Cu particle into the polydimethylsiloxane (PDMS) matrix as an elastomer and developed flexible PZL rubber. The H-ZnS:Cu powder shows typical wurtzite structure without secondary phase (Figure 2a) after hydrogenation treatment. Figure 2b shows microstructure of the PZL rubber with well-dispersed H-ZnS:Cu particles in the PDMS matrix. The PZL rubber emitted green light under periodic stretching motion and the intensity of the emitted light is maximized with optimum volumetric contents of the ZnS:Cu particles in PDMS elastomer (PDMS:ZnS:Cu=2:1). Figure 3a shows the PZL spectra obtained from each composition with different hydrogenation conditions for the H-ZnS:Cu microparticles. The PZL intensity was linearly increased with increasing hydrogenation temperature up to 250°C. We found significantly enhanced PZL intensity at the optimum hydrogenation condition (250°C). The results indicated that the defect state and sulfur vacancy formation are directly related to magnitude of intensity of light emission and controlling concentration of sulfur vacancies is an effective method for enhancing the PZL effect. Our PZL rubber is much easier to be integrated with various applications due to its stretchability and a simple manufacturing process. For example, we have demonstrated a PZL glove (Figure 3b) by using PZL paste. We applied PZL paste on cotton glove and solidified it *via* curing. The PZL rubber coated glove maintains its shape during gripping-releasing motion.

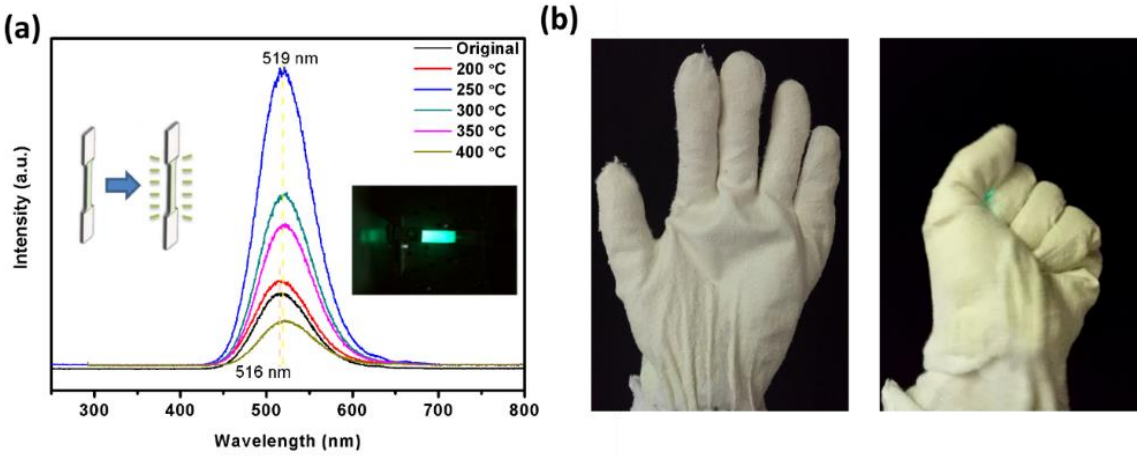

Figure 3. (a) Luminescence spectroscopy of PZL rubbers under different hydrogenation temperatures and periodic stretching-releasing motion. (b) Picture of PZL glove: releasing and gripping.

In order to understand the chemical composition and defect state of H-ZnS:Cu microparticles, X-ray photoelectron spectroscopy (XPS) analysis was performed. Figure 4a displays the Zn $2p_{3/2}$ core level spectrum of six H-ZnS:Cu particles. A perfect fit to the peak located at 1022.8 eV was obtained corresponding to the characteristic spin-orbit $2p_{3/2}$. [6-8] This result indicates that zinc valent state is mainly +2 in the particles. As the hydrogenation temperature was increased, the Zn $2p_{3/2}$ line of H-ZnS:Cu showed a peak shift of 0.35 eV towards lower binding energy in comparison to those of ZnS, suggesting the reduction of Zn^{2+} to lower oxidation states.[9] The peaks located at 1020 eV were found to correspond to the trace Zn^0 at the surface of metal sulfides.[8] For the sample treated at higher temperature, the peak area at 1020 eV was found to be different, corresponding to the ratio of 0:674:687:741:834:858 from room temperature to 400 °C respectively. The surface average oxidation states for H-ZnS:Cu powders were calculated to be 2, 1.75, 1.72, 1.65, 1.58, and 0.8, respectively, with increasing temperature.[10] Sulfur non-stoichiometry in H-ZnS:Cu resulted from heat treatment under hydrogen atmosphere as the formation of sulfur deficiencies is an endothermic process. The lower average surface oxidation state for the H-ZnS:Cu powder reflects the compensation of sulfur vacancies by reduction of Zn. This result indicates that surface of H-ZnS:Cu powder has non-stoichiometric formulation, ZnS_{1-x}, and higher hydrogenation temperature promotes the formation of vacancies.

Raman spectra of ZnS and H-ZnS:Cu samples were also collected to investigate the effect of thermal hydrogenation treatment (Figure 4b). All the Raman peaks can be indexed to the characteristic first and second order Raman peaks of wurtzite ZnS, indicating that as-prepared particles exhibit asymmetric wurtzite structure,[11, 12] belonging to the space group C_{6v} (6mm) in primitive cell. For such a structure, the following vibration modes correspond to:[11] $\Gamma_{opt}=A_1+E_1+2E_2+2B_1$. The B_1 modes are silent modes, A_1 and E_1 modes are polar modes and both are Raman and infrared active, while E_2 modes are nonpolar and Raman active. The distinctive peak at 350 cm^{-1} is assigned to the A_1(LO) vibration mode. The TO overtones at L and X points[13] can be found at 618 and 643 cm^{-1} in the high-frequency region, respectively. The LO overtone at Γ is found at 677 cm^{-1}. Note that A_1(LO) phonon mode corresponds to atomic oscillations along the c-axis; thus, the peak value of this mode is sensitive to lattice strain. The characteristic Raman peaks of the H-ZnS:Cu samples show a red shift and broadened peaks with increasing temperature, suggesting an increased lattice strain produced by sulfur vacancies after hydrogenation (Figure 4c).[14, 15]This result is consistent with the XPS analysis confirming that ZnS:Cu hydrogenated at higher temperature possesses higher fraction of sulfur vacancies.

The UV-visible absorption spectra of raw ZnS:Cu and H-ZnS:Cu samples were collected to investigate the influence of hydrogenation on the optical absorption (Figure 4d). All samples exhibited similar light absorption in the UV region. In comparison to unmodified ZnS:Cu, a clear red-shift of the absorption edge can be observed for all H-ZnS:Cu samples. Interestingly, the absorption edge of H-ZnS:Cu was shifted towards the visible region and the sample annealed at 400°C shows substantially higher absorption in the region of 450-600 nm. The optical band gap (E_g) of a semiconductor material can be calculated from the Tauc equation,[16] $(\alpha h\nu)^2=A(h\nu - E_g)$, where $h\nu$ is the photon energy, α is the absorption coefficient, and A is a constant for the material. From Figure 4e, the calculated direct E_g values for H-ZnS:Cu are 2.87, 2.85, 2.84, 2.81, 2.79, and 2.75 eV from original to 400 °C annealed samples, which are smaller than values for bulk ZnS (3.65 eV). This is related to absorption at longer wavelength from Cu^{2+}. The red-shift phenomenon of the UV absorption spectra can be elucidated by the presence of defects,[17, 18] which is caused by the valence transition of Zn ions. These results further confirm that the number of sulfur vacancies in ZnS and impurity states were introduced in the band-gap of ZnS during hydrogenation.

From the results, we found that the 400 °C sample contains a higher density of defect states and sulfur vacancies. The enhanced PZL performance of H-ZnS:Cu microparticles can be attributed to the increased number of sulfur vacancies after hydrogenation, which provide free electrons that play role as trap centers. The luminescence properties are closely related to the collection of excited electrons, electron energy transition, and recombination reactions. However, the 400 °C sample did not exhibit the best PZL property. From this, we could hypothesize that there is an optimum defect concentration to maximize the PZL intensity. In order to validate our hypothesis, we used a steady state fluorescence spectrometer to investigate the room temperature photoluminescence (PL) spectra of samples, as shown in Figure 4f. All the samples had a strong and sharp PL emission centered at c.a. 510 nm. The red shift is due to the structural change and defect state formed after hydrogenation. There are two broad emission categories: the near-band-edge (NBE) emissions and deep level (DL) emissions. The NBE emissions are favored by the high crystal quality and quantum confinement effect, and the DL emissions can be enhanced by impurities, or structural defects of the crystal [19]. The 510 nm emission at room temperature is mainly attributed to the sulfur vacancies and defect states of ZnS, which may lead to high DL-emissions to-NBE-emissions ratio [20, 21]. The intensity trend is the same as observed with the PZL results (Figure 2a), whereby the 250 °C sample shows the most effective emission and least thermal radiative recombination (TRR) energy loss.

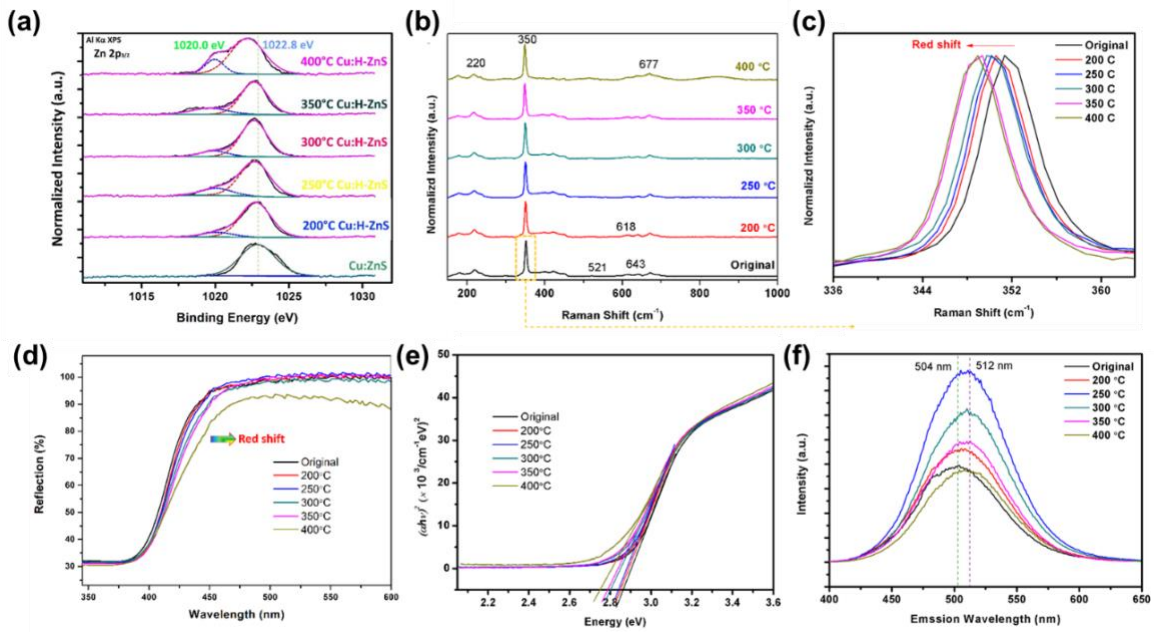

Figure. 4 (a) Normalized Zn $2p_{3/2}$ core level XPS spectra collected for ZnS:Cu and H-ZnS:Cu powders at different hydrogenation temperatures. (b) Normalized Raman spectra of ZnS:Cu and H-ZnS:Cu powders at different hydrogenation temperatures. (c) High resolution normalized Raman spectra for all H-ZnS:Cu powders obtained at 335-365 cm^{-1}. (d) Optical absorption spectrum and (e) $(\alpha hv)^2$ vs hv curves for ZnS:Cu and H-ZnS:Cu powders at different hydrogenation temperatures. (f) Room temperature photoluminescence spectra of as-prepared ZnS:Cu and H-ZnS:Cu powders produced at different hydrogenation temperatures with the excitation wavelength of 370 nm.

The PZL performance recorded from the samples indicates that sulfur vacancies and defect states have a two-pronged effect on the electron energy transition and recombination process. First, sulfur vacancies ($V_S^{\cdot\cdot}$) are surrounded by Zn^{2+} ion 2s orbitals that are stabilized from the Zn 2s band due to lack of covalent bonding with the missing S^{2-} ion; therefore, symmetrical Zn 2s orbitals at each V_s form shallow donor state levels [22] just below E_c that accommodate two electrons per sulfur vacancy. Thus, the shallow donor state originating from Zn 2s orbitals is created by loss of sulfur atoms, which creates a new vacancy level. Therefore, the vacancies injected during the synthesis process can act as donors and induce the formation of new energy levels in the band gap. We provide a simplified band energy diagram illustrating the electron energy transition in different H-ZnS:Cu microparticles which facilitates the comparative analysis. According to Haranath *et al.*,[23] the PZL green light emission is related to the electron energy transition from conduction band of ZnS to Cu^{2+} center. As illustrated in Figure 5, in the band structure, a new level is induced by $V_S^{\cdot\cdot}$ that promotes the generation of trapped electrons.[15] When stress is applied, piezoelectric charges are created within ZnS. The conduction and valence bands of ZnS are tilted due to the potential produced by the piezoelectric field under the applied mechanical stress. As a result, a larger number of trapped electrons in the upper defect state become available and this in turn increases the probability to be detrapped and released into the conduction band [24]. In this scenario, non-radioactive recombination (NRR) occurs between released electrons from new defects and holes, transferring energy (≈2.5 eV) to the Cu^{2+} ion and exciting its outer shell electrons (required energy 2.2–2.4 eV), controlling the emission intensity. An increased concentration of sulfur vacancies results in a higher density of detrapped electrons for recombination, which provides higher energy for activating Cu^{2+}. When more excited electrons of Cu^{2+} ions fall back to the ground state, intense green color light is emitted. We hypothesize that excess defects act as the electron recombination centers that reduces the emission intensity. Increasing the concentration of vacancies above

threshold value results in more excited electrons getting trapped. Some fraction of the available electrons will act as NRR centers and transfer the energy to Cu^{2+} ions for excitation. Other trapped electrons will go through radioactive recombination and release the energy through the thermal emission process.[25] Thus, there exists an optimum balance. While TRR has a larger scale than NRR energy transfer, there will be a diminishing PZL light emission due to less availability of excited Cu^{2+}. The former has higher probability in materials with an excess number of defects.[26-28] Therefore, the sample annealed at 250°C has the optimum number of defects with trapped electrons that can effectively undergo NRR, indicating that it has the best NRR to TRR ratio.

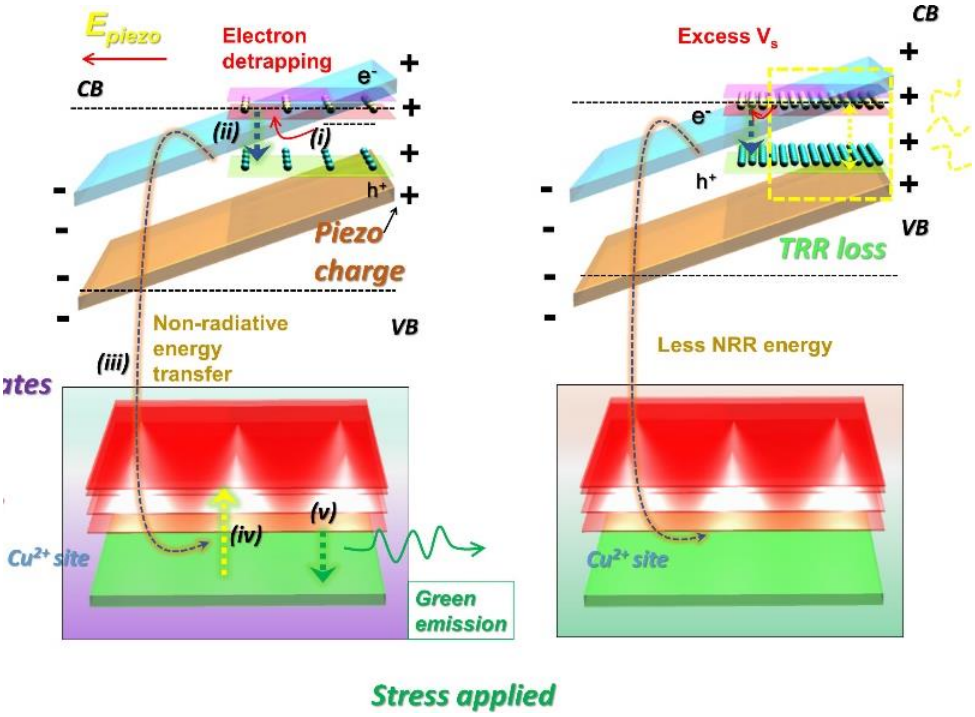

Figure 5 The piezoluminescence effect initiates the emission process: the case with optimum amount of $V_S^{\cdot\cdot}$ (left) and the case with excess $V_S^{\cdot\cdot}$ (right).

(b) <u>*Study of piezoelectric potential on PZL intensity –*</u> Besides the physical properties of ZnS that determines the PZL performance of elastomers, sample configuration is also important, because higher applied stress results in higher PZL intensity. For better understanding of the PZL mechanism, we have investigated the relationship between applied stress and piezoelectric potential through numerical simulation using COMSOL. For this simulation, we assumed 25 µm-diameter ZnS particles are well-dispersed in the PDMS elastomer of 28.5 µm × 28.5 µm × 161.1 µm volume. The internal stress profile and induced electrical potential were calculated when 10% strain was induced in PZL elastomer along length direction. Figure 4 shows internal stress (left) and electrical potential (right) profiles with different ZnS content. The stress and electric potential in PZL elastomer increases with increasing ZnS content. The trend of stress change between ZnS particles is very close to the experimental result in the mechano-stretch test under 10% strain (Figure 6). The induced stress exponentially increases near 100:45 composition in simulation (Figure 7a). However, we found that the stiffness of PZL elastomer is increased with increasing volume ratio of ZnS:Cu particles up to 100:50 composition and after that the stiffness starts to dramatically decrease to lower value in experimental results (Figure 7b). This may be because the induced stress exceeds tensile strength of the PDMS (5.13 MPa) polymer near 100:60 composition leading to breakage of links between ZnS particles. These inside cracks are generated in PZL elastomer after several stretching-releasing test cycle that decreases the stiffness of PZL elastomer. The induced electric potential, which is the driving force to excite trapped electrons, exhibits similar trend with applied stress in ZnS

interior. This result is well aligned with piezoelectric theory, since the electric field and stress exhibit linear relationship following relation $E=gX$ where, E, g, and X are electric field, piezoelectric voltage constant, and applied stress, respectively (Figure 7c). In the same way, PZL intensity of the elastomers trends with stiffness, because different stiffness results in variation of stress applied on ZnS:Cu particles under same strain. (Figure 7d). This is important observation as it provides data on balancing the particle-particle contact with the stiffness of the matrix. During this program, we will utilize the contact theory and micromechanics models to understand the nature of particle-particle contact and its influence on light emission.

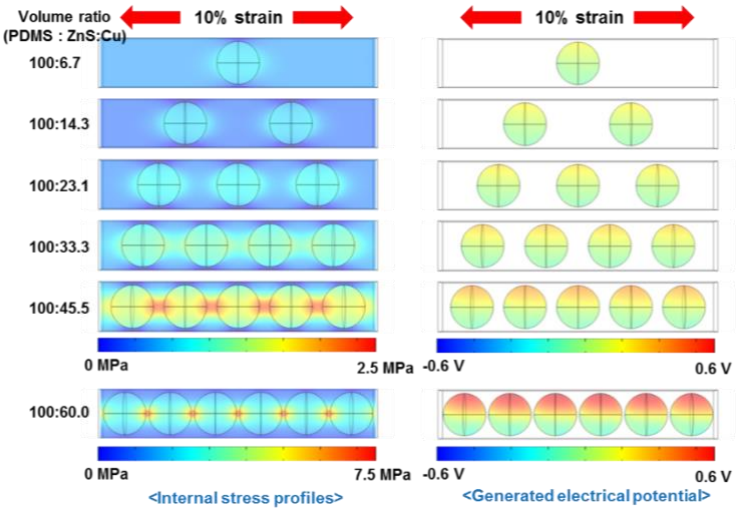

Figure 6. Numerical simulation for stress induced electric potential in PZL elastomer with varying ZnS content

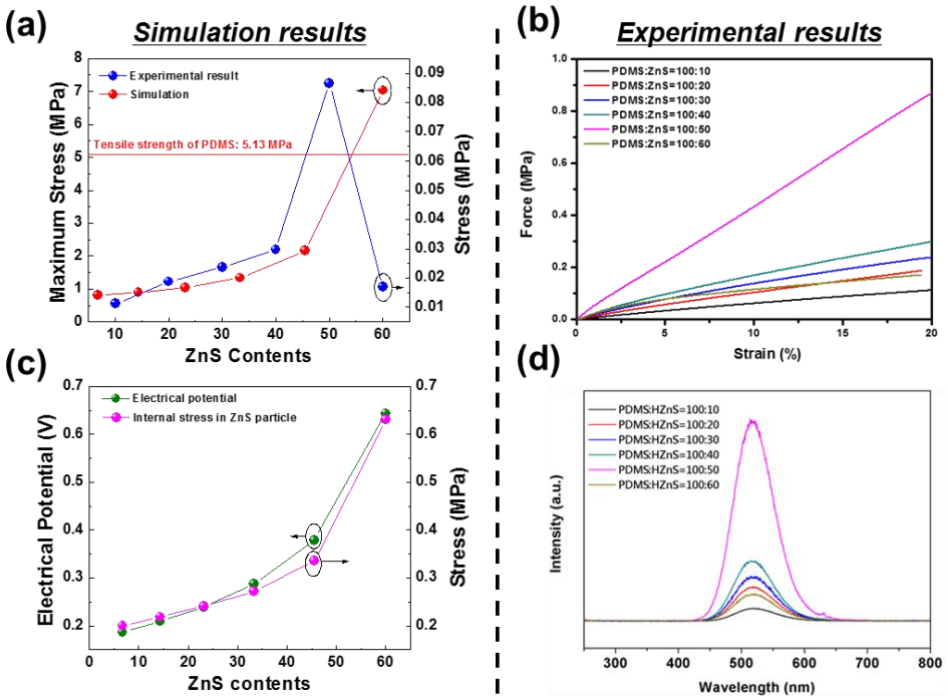

Figure 7. (a) Simulation results of internal stress in PZL elastomers with different PDMS:ZnS:Cu volume ratio (b) Mechano-stiffness test on PZL elastomer samples with different PDMS:ZnS:Cu volume ratios (100:10 to 100:60). The measured size of each sample is 1 cm × 3 cm × 0.1 cm (width, length, thickness). (c) Simulation results of internal piezoelectric petential in PZL elastomers with

(c) Applications

The PZL rubbers emitted green light under periodic stretching motion and the intensity of the light was maximized at optimum volumetric content of the ZnS:Cu particles in PDMS elastomer (PDMS:ZnS:Cu=2:1) (Figure 8a). Furthermore, we developed flexible electroluminescence light emitting rubber with different color (Figure 8b) using this technique. Our PZL rubber technique can be easily applied on various applications due to its stretchability and simple manufacturing process. For example, we have demonstrated a PZL writing pad (Figure. 8c) by using PZL composite paste. The pad enables tracking of the writing motion and is detectible with wireless sensors (eg. photodiode arrays). Our PZL rubbers provides various emission color (green, blue, orange, white, etc) by controlling doping level of the Cu dopant. For future applications, we have demonstrated PZL sensing gloves with various color (Figure 8d). The PZL rubbers were attached at the joints of fingers and luminescence was observed during gripping-releasing motion. The intensity of the PZL was varied with different deformation and motion speed of the fingers, which is a promising behavior for the non-contact strain sensor and motion information devices.

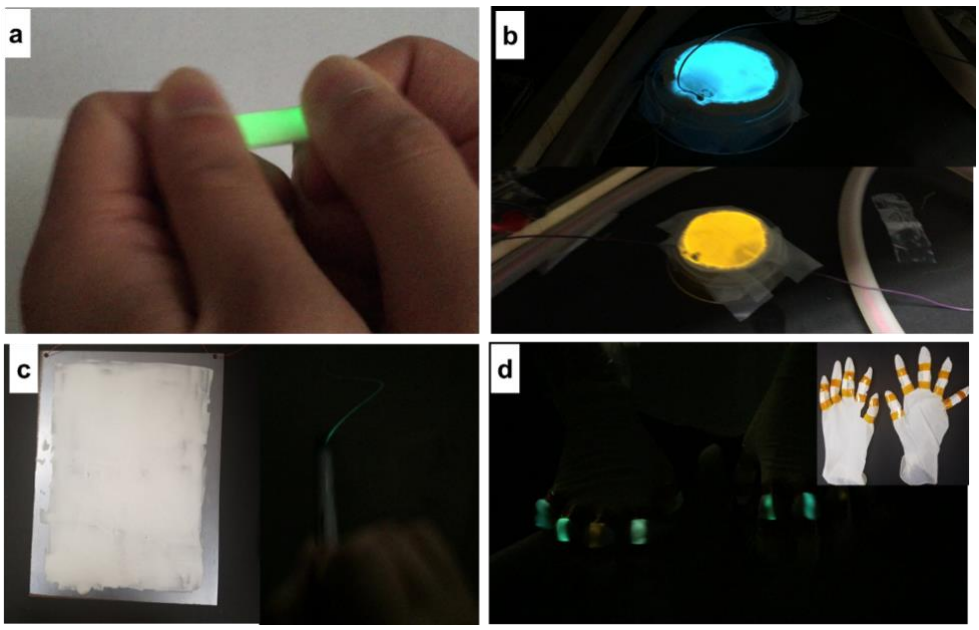

Figure 8. Applications of PZL elastomer. (a) light emission from PZL elastomer under stretching motion (b) flexible electroluminescence light emitting rubber with different color (c) PZL writing pad (d) PZL gloves

(d) Technology transfer

A great merit of the PZL composite is that we can synthesize it in the desired form factor. Optical fiber composite with PZL is one of the promising strain/damage detection system in structures and wearable kinesiological sensors, etc. We have initiated collaboration on PZL particles and composite processing technique with Dr. Wetzel at Army Research Laboratory (ARL) for developing novel PZL optical fiber. ARL has an outstanding technique to fabricate glass and polymer optical fiber using thermal drawing process (TFD, Figure 9 (left)), which has advantages in achieving high microstructural complexity with short lead time. Our goal is to realize stretchable and flexible optical wave guide fiber containing PZL particles. As the fiber is deformed (stretching, compressing, bending, vibrations. etc.), luminescence occurs and the light concentrates through internal reflection sending most of the generated photons through the fiber ends. Dr. Wetzel's team has initiated PZL polymer fiber synthesis using our hydrogenated ZnS:Cu particles. The light intensity was shown to be higher in the PZL composite (Figure 9(right)).

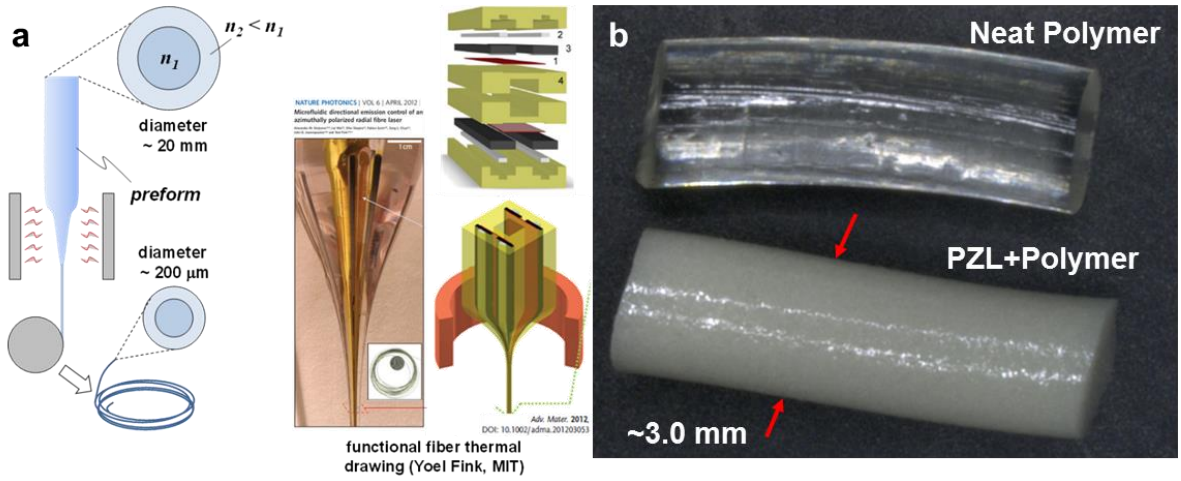

Figure 9. (a) Schematic of optical fiber and thermal drawing process technique (b) PZL polymer fiber.

3. Bibliography

[1] X. D. Wang, H. L. Zhang, R. M. Yu, L. Dong, D. F. Peng, A. H. Zhang, Y. Zhang, H. Liu, C. F. Pan, Z. L. Wang, *Advanced Materials* **2015**, *27*, 2324.

[2] S. M. Jeong, S. Song, S. K. Lee, N. Y. Ha, *Advanced Materials* **2013**, *25*, 6194.

[3] S. M. Jeong, S. Song, K. I. Joo, J. Kim, S. H. Hwang, J. Jeong, H. Kim, *Energy & Environmental Science* **2014**, *7*, 3338.

[4] N. Terasaki, H. Zhang, H. Yamada, C.-N. Xu, *Chemical Communications* **2011**, *47*, 8034.

[5] C. N. Xu, T. Watanabe, M. Akiyama, X. G. Zheng, *Applied Physics Letters* **1999**, *74*, 1236.

[6] W. Liu, *Materials Letters* **2006**, *60*, 551.

[7] T. Ben Nasrallah, M. Amlouk, J. C. Bernede, S. Belgacem, *Physica Status Solidi A: Applied Research* **2004**, *201*, 3070.

[8] D. Chadwick, T. Hashemi, *Corrosion Science* **1978**, *18*, 39.

[9] T. L. Barr, J. J. Hackenberg, *Applied Surface Science* **1982**, *10*, 523.

[10] F. Xiao, Y. L. Xu, *International Journal of Electrochemical Science* **2012**, *7*, 7440.

[11] Y. C. Cheng, C. Q. Jin, F. Gao, X. L. Wu, W. Zhong, S. H. Li, P. K. Chu, *Journal of Applied Physics* **2009**, *106*.

[12] J. H. Kim, H. Rho, J. Kim, Y. J. Choi, J. G. Park, *Journal of Raman Spectroscopy* **2012**, *43*, 906.

[13] W. G. Nilsen, *Physical Review* **1969**, *182*, 838.

[14] G. Wang, Y. Ling, H. Wang, X. Yang, C. Wang, J. Z. Zhang, Y. Li, *Energy & Environmental Science* **2012**, *5*, 6180.

[15] J. Gan, X. Lu, J. Wu, S. Xie, T. Zhai, M. Yu, Z. Zhang, Y. Mao, S. C. Wang, Y. Shen, Y. Tong, *Sci Rep* **2013**, *3*, 1021.

[16] X. H. Lu, X. Huang, S. L. Xie, D. Z. Zheng, Z. Q. Liu, C. L. Liang, Y. X. Tong, *Langmuir* **2010**, *26*, 7569.

[17] P. Patsalas, S. Logothetidis, C. Metaxa, *Applied Physics Letters* **2002**, *81*, 466.

[18] M. Y. Chen, X. T. Zu, X. Xiang, H. L. Zhang, *Physica B-Condensed Matter* **2007**, *389*, 263.
[19] W. S. Seo, H. H. Jo, K. Lee, J. T. Park, *Advanced Materials* **2003**, *15*, 795.
[20] Y. C. Kong, D. P. Yu, B. Zhang, W. Fang, S. Q. Feng, *Applied Physics Letters* **2001**, *78*, 407.
[21] D. M. Bagnall, Y. F. Chen, Z. Zhu, T. Yao, M. Y. Shen, T. Goto, *Applied Physics Letters* **1998**, *73*, 1038.
[22] G. M. Wang, H. Y. Wang, Y. C. Ling, Y. C. Tang, X. Y. Yang, R. C. Fitzmorris, C. C. Wang, J. Z. Zhang, Y. Li, *Nano Letters* **2011**, *11*, 3026.
[23] K. Jayanthi, S. Chawla, H. Chander, D. Haranath, *Crystal Research and Technology* **2007**, *42*, 976.
[24] D. O. Olawale, T. Dickens, W. G. Sullivan, O. I. Okoli, J. O. Sobanjo, B. Wang, *Journal of Luminescence* **2011**, *131*, 1407.
[25] W. Vanroosbroeck, W. Shockley, *Physical Review* **1954**, *94*, 1558.
[26] P. M. Smiley, R. N. Biagioni, A. B. Ellis, *Journal of the Electrochemical Society* **1984**, *131*, 1068.
[27] S. Hu, C. X. Xiang, S. Haussener, A. D. Berger, N. S. Lewis, *Energy & Environmental Science* **2013**, *6*, 2984.
[28] H. Doscher, J. F. Geisz, T. G. Deutsch, J. A. Turner, *Energy & Environmental Science* **2014**, *7*, 2951.

4. Appendixes

List of Publication

1. Jiayong Gan, Min Gyu Kang, Michael A Meeker, Fiti A. Khodaparast, Robert J. Bonnar, James E. Mahaney, Deepam Maurya, and Shashank Priya, "Enhanced piezoluminescence in non-stoichiometric ZnS:Cu microparticle based light emitting elastomers" ***Journal of Materials Chemistry C***, **Vol. 5,** 5387 (05/12/2017)